Stem Cell Reports, Volume *7*

Supplemental Information

L-*MYC* Expression Maintains Self-Renewal and Prolongs Multipotency of Primary Human Neural Stem Cells

Zhongqi Li, Diana Oganesyan, Rachael Mooney, Xianfang Rong, Matthew J. Christensen, David Shahmanyan, Patrick M. Perrigue, Joseph Benetatos, Lusine Tsaturyan, Soraya Aramburo, Alexander J. Annala, Yang Lu, Joseph Najbauer, Xiwei Wu, Michael E. Barish, David L. Brody, Karen S. Aboody, and Margarita Gutova

Supplemental Experimental Procedures

Cytotoxicity assays

Human U251 glioma cell line was used in *in vitro* cytotoxicity assays as described previously (Metz et al., 2013). Briefly, cells were placed into 96-well plates (5,000 cells per well, in triplicate) in 100 ml of culture media per well and cultured for 24 hours. Irinotecan (CPT-11), diluted in control culture medium or conditioned medium from CE-expressing LM-NSC008 cells, was then added to final concentrations of 0-100 μM. Cells were incubated with irinotecan for 4 hours, after which medium was aspirated and replaced with drug-free fresh medium, and cells were grown for an additional 96 hours. Characterization of the toxic effect of CPT-11 and CPT-11 in combination with hCE1m6 on U251 glioma cells was performed using the CellTiter-Glo® Luminescent Cell Viability Assay to measure ATP activity as an indicator of cell viability (Promega, G7571). Mean values ± SD of three independent experiments in triplicate measurements are shown. Multiple t-test analysis (Prism Version 6) with Holm-Sidak adjustment for multiple comparisons was performed to analyze significant differences among CPT-11 and CPT-11+CE treated samples for each CPT-11 concentration (0-100 μM). $P < 0.0001$ values for (0.5-100 μM).

Colony formation assay

A standard soft agar colony formation assay was used to assess anchorage-independent NSC growth *in vitro*. Human tumor cells (5637 bladder and MCF7 breast, ATCC) and LM-NSC008 (p12), HB1.F3.CDs (p28) were encapsulated at 1 x 10^5 cells/ml within 50 μl of 1% w/w agarose hydrogels cured in a 96-well plate. Gels were labeled with Calcein-AM (Life Technologies) and imaged using a confocal microscope (Zeiss Axial observer Z1) after culture for 7 days in complete growth media. ImageJ was used to count and measure sizes of cells and cell clusters present in Z-axis projections of 13 optical sections spaced 100 μm apart.

Imunohistochemistry (IHC) and immunocytochemistry (ICC)

Paraffin-embedded brain sections (10 μm) were processed for histological staining for H&E (hematoxylin eosin). Immunostaining was performed using anti eGFP (Abcam 290, 1:500 dilution), TUNEL (ApopTag® Peroxidase In Situ Apoptosis Detection Kit cat. # S7100, Millipore), anti Ki-67 (Chemicon, MAB4062, at 1:25 dilution), anti Human Nestin (Chemicon MAB5326 at 1:100 dilution) and anti L-myc (Santa Cruz Biotechnology, Inc. SC-28699, at dilution 1:100) antibodies. Immunoreactivity was visualized using Thermo Scientific Pierce DAB Substrate Kit which enables chromogenic detection of horseradish peroxidase (HRP) activity based the action of 3,3'-diaminobenzidine (DAB).

For cell differentiation experiments, primary human NSC008s and LM-NSC008 cells were cultured in DMEM supplemented with 1% fetal bovine serum (FBS). After 10 days, cells were fixed with 4% paraformaldehyde (PFA) for 4 min and washed in phosphate buffered saline (PBS) twice. Fixed cells were stained using standard ICC protocol using the following antibodies: 1) Class III β-Tubulin ((TUJ1) MMS435P, Covance Inc., at dilution 1:2000); 2) SOX9 (AF3075, R&D Systems Inc., at dilution 1:20); 3) GFAP (SMI-21R, Covance, at 1:1000 dilution); 4) human GFAP (Stem123, Y40420,Takara Bio Inc., at dilution 1:1000); 5) O4 (MAB1326, R&D Systems Inc. at dilution 1:100).

Flow cytometry analysis of primary NSC008 and LM-NSC008 cells

Cells were harvested at passage 8, washed and incubated with antibodies in room temperature for 30 minutes using staining buffer (PBS + 1% FBS). Unstained cells or cells stained with IgG isotype control antibodies were used as negative controls. Acquisition and analysis was performed on a Guava Express Plus $^{3.1}$ and software. Concentrations of antibodies used for flow cytometry were as follow: 1) SOX2 (FCMAB112F, Millipore Corp., at dilution 1:100); 2) OCT4 (FCMAB113A4, Millipore Corp., at dilution 1:100); 3) Nestin (IC1259F, R&D Systems, at dilution 1:20); 4) A2B5(MAB1416, R&D Systems, 2.5 mg/10^6 cells); 5) CD133 (130-080-801, Miltenyi Biotech, at dilution 1:11), and 6) Olig 1, 2, 3 (IC2230P, R&D Systems, at dilution 1:20). RNA-Seq data is provided to support flow cytometry results for expression level of SOX2, PAX6 and OCT4 genes (Table S3).

mRNA deep sequencing with Illumina Hiseq2500

Sequencing libraries were prepared with the TruSeq RNA Sample Preparation Kit V2 (Illumina) according to the manufacturer's protocol with minor modifications. Briefly, 500 ng of total RNA from each sample was used for polyadenylated RNA enrichment with oligo dT magnetic beads, and the poly (A) RNA was fragmented with divalent cations under elevated temperature. First-strand cDNA synthesis produced single-stranded DNA copies from the fragmented RNA by reverse transcription. After second-strand cDNA synthesis, the double-stranded DNA underwent end repair, and the 3′ ends were adenylated. Finally, universal adapters were ligated to the cDNA fragments, and 10 cycles of PCR were performed to produce the final sequencing library. Library templates were prepared for sequencing using the cBot cluster generation system (Illumina) with TruSeq SR Cluster V3 Kit. Sequencing runs were performed in single read mode of 51 cycle of read1 and 7 cycles of index read using Illumina HiSeq 2500 platform with TruSeq SBS V3 Kits. Real-time analysis software was used to process the image analysis and base calling. Sequencing runs generated approximately 40 million single reads for each sample.

RNA-Seq data analysis

The 51-bp-long single-ended sequence reads were mapped to the human genome (hg19) using TopHat, and the frequency of Refseq genes was counted using customized R scripts. The raw counts were then normalized using the trimmed mean of M values (TMM) method and compared using Bioconductor package "edgeR" (Robinson et al., 2010). Reads per kilobase per million (RPKM) mapped reads were also calculated from the raw counts. Differentially expressed genes were identified if RPKM ≥ 1 in at least one sample, fold change ≥ 3, and $P \leq 0.05$. Gene enrichments were analyzed using DAVID (National Institute of Allergy and Infectious Diseases (NIAID), 2016). Hierarchical clustering analysis was performed in cluster 3.0 using the average linkage clustering method (Wilson et al., 2004). The results were then visualized in Treeview and a heatmap was generated (Saldanha, 2004). Differentially expressed (DE) gene lists from the group comparison mentioned above were uploaded to DAVID v6.7 (Dennis et al., 2003) to identify enriched biological themes particular for GO terms and KEGG pathway (Tables S1, S2). Complete gene list of functional pathways is provided as Table S5.

Whole exome sequencing for somatic mutations and copy number variation analysis

Coding exons from genomic DNA samples were amplified using the Ion Ampliseq Exome kit (Catolog number 4487084, ThermoFisher Scientific Inc.). The amplified products were loaded onto the Proton Q1 chip and sequenced using Ion Proton sequencer following manufacturer's recommendations. For each sample, about 25 million reads were generated, which provided coverage of 52x for P2 cells and 64x for P12 cells for the coding exons. DNA

sequences were aligned to hg19 with Torrent Suite TMAP. Somatic mutations were identified using VarScan (Koboldt et al., 2012) and further filtered to remove false positives with the following criteria: 1) allele total coverage in P12 > 10; 2) alternative allele frequency in P12 >= 25%; 3) Alternative allele is not detectable in P2 sample. Copy number variation analysis was performed as described previously (Zhang et al., 2013). Briefly, exon level coverage for each coding exon in the RefSeq genes were counted using custom R scripts and Bioconductor package "ShortRead" and "Granges". Copy number variation was detected using R package "DNAcopy" with log2 fold change of exon level coverage between the two cell types LM-NSC008-p12 vs p2 (Table S4).

Supplementary Figures and Tables

A

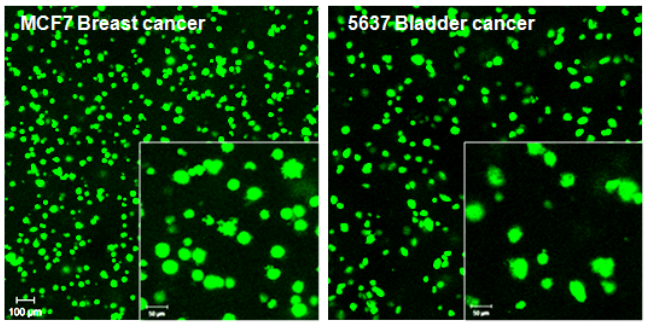

B

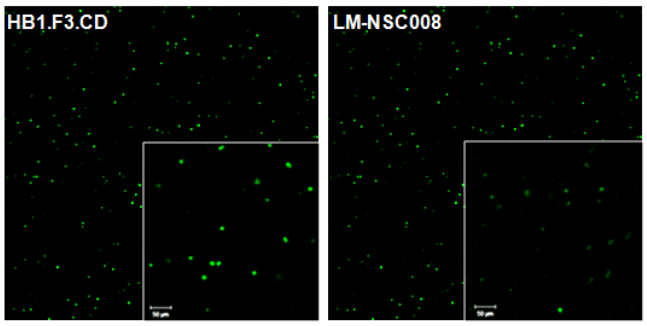

C

Cell line	Viable as single cells (%)	Colony-forming efficiency (%)
LM-NSC008 (p12)	**1.6 ± 0.7**	**0.0 ± 0.0**
HB1.F3.CD (p28)	**3.0 ± 0.3**	**0.0 ± 0.0**
MCF7 breast cancer	**7.1 ± 0.6**	**32.1 ± 2.5**
5637 bladder cancer	**1.1 ± 0.5**	**21.1 ± 2.4**

Figure S1. *In vitro* tumorigenicity of neural stem cells. LM-NSC008 and HB1.F3.CD NSCs did not form colonies characteristic of cancer cells when cultured for 7 days in soft agar (B), in contrast to MCF7 breast cancer and 5637 bladder cancer cells (A). Shown are representative maximum intensity projections of confocal microscope z-stacks obtained on day 7 after calcein-AM labeling. Scale bar = 100 µm for all images and 50 µm for all insets. (C) Table of data obtained using ImageJ analysis software to count and size colonies in 5 images per condition in 2 independent experiments. Colonies were defined as clusters with diameters >20 µm.

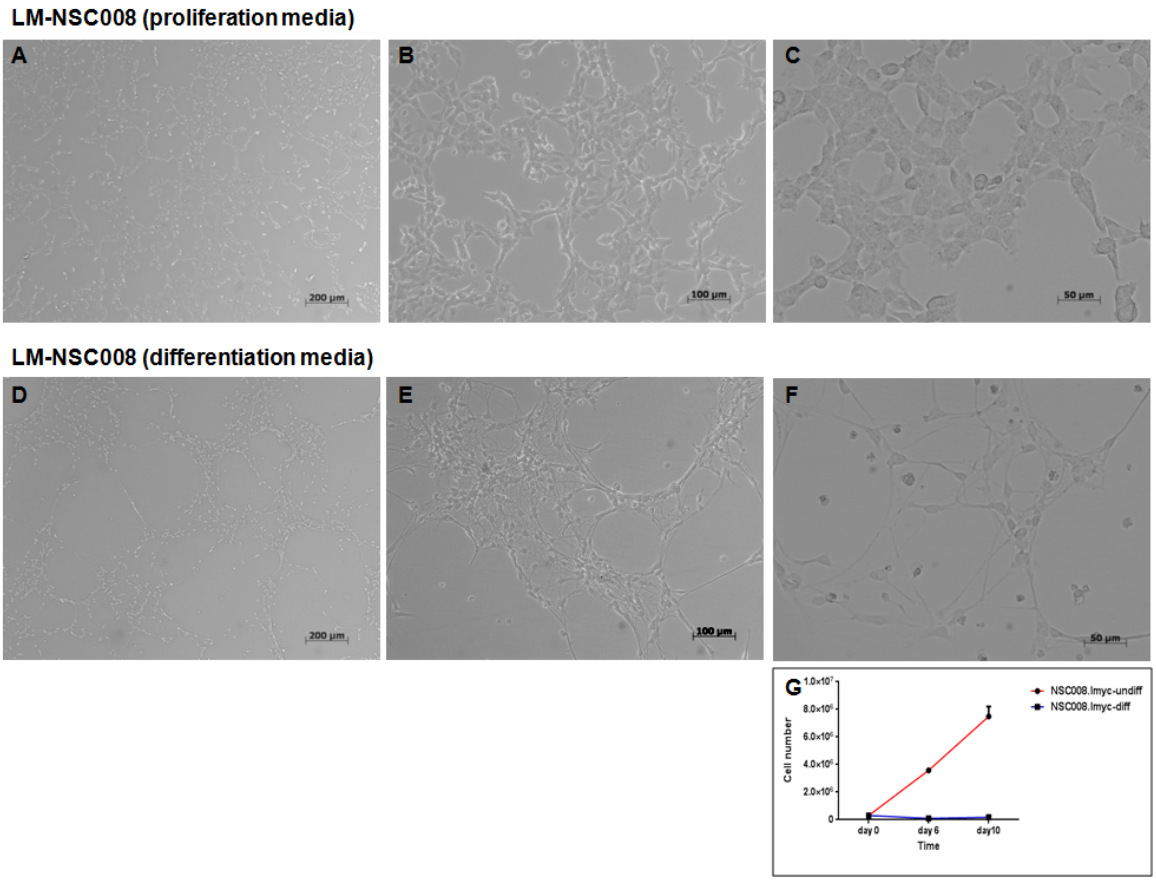

Figure S2. Proliferation and differentiation of LM-NSC008 cells *in vitro.* Bright-field images of LM-NSC008 cells in culture. (A-C) LM-NSC008 cells (p6) grown in proliferation media (NSC media/with EGF and FGF, day 4). (D-F) LM-NSC008 cells grown in differentiation media (NSC media with 1% fetal bovine serum, day 4). Scale bars 200, 100, 50 µm. (G) Growth kinetics of LM-NSC008 cells cultured in proliferation and differentiation media for 10 days. Mean values ± SD of two independent experiments in triplicate measurements are shown.

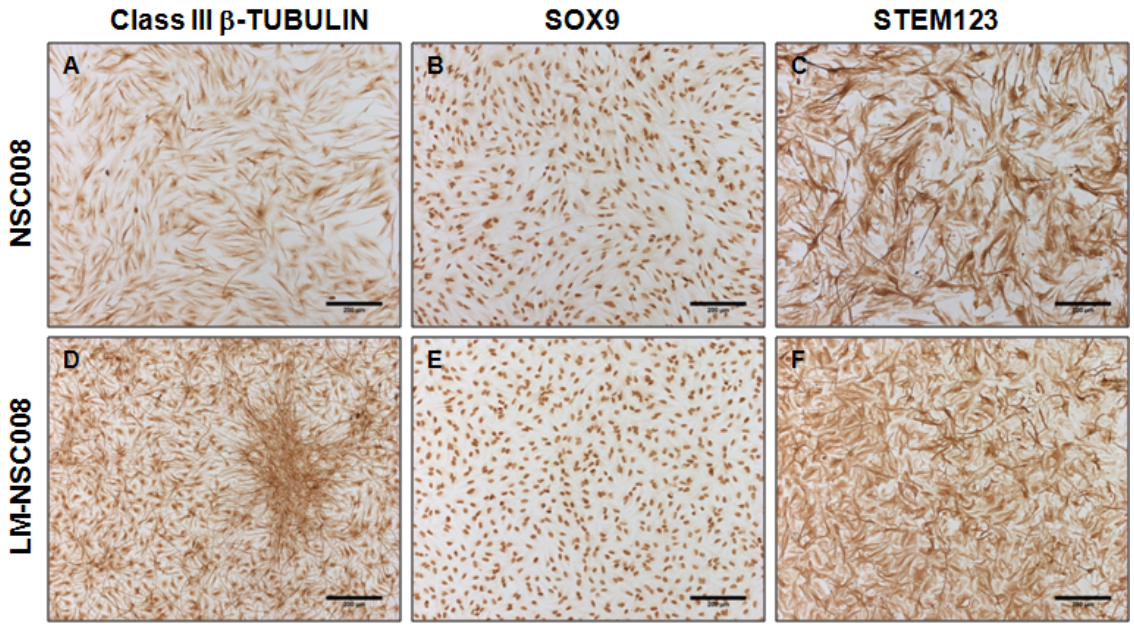

Figure S3. Figure S3. Immunocytochemistry for differentiation markers was performed for untransduced hNSCs and L-myc transduced LM-NSC008 lines after differentiation for 10 days. (A, B, C) ICC of hNSCs after differentiation using antibodies for Class III β-TUBULIN (TUJ1), SOX9 and STEM123 detection (10x bright field images). (D, E, F) ICC of LM-NSC008 cells using the same antibodies (10x images). Scale bars, 200 μm.

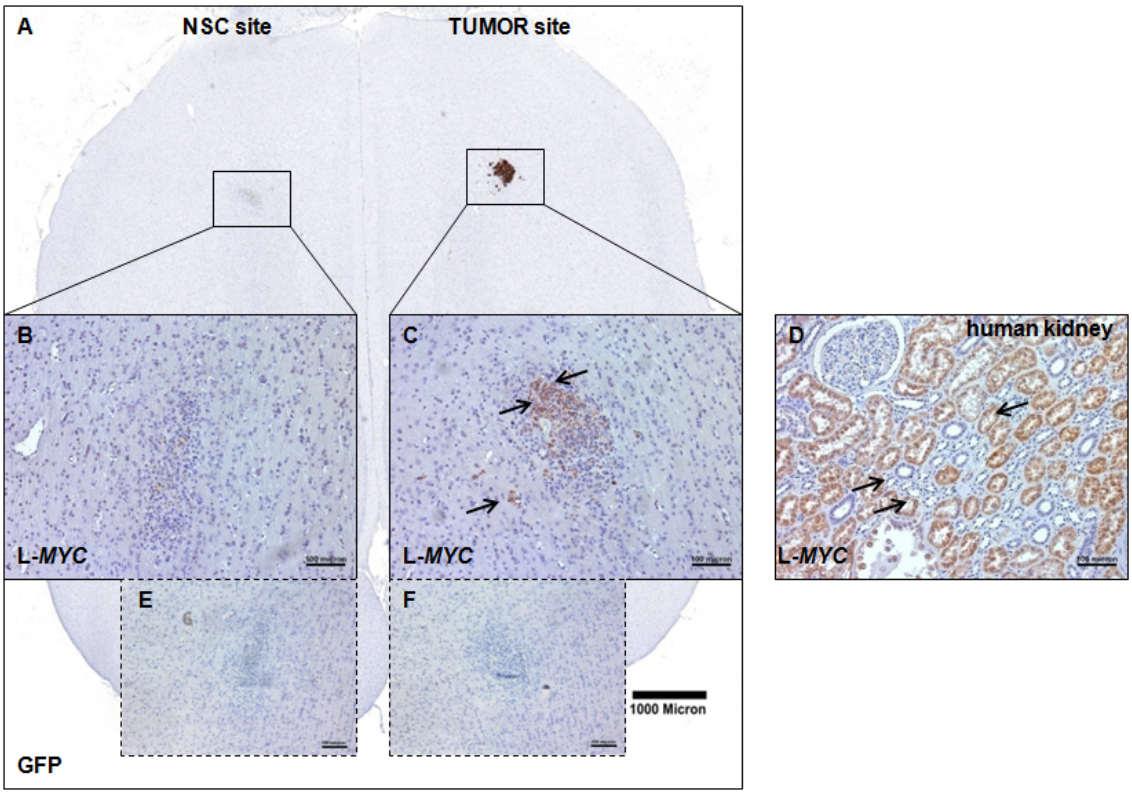

Figure S4. L-myc staining of brain sections. Adult NSG mice were implanted intracranially with U251.eGFP human glioma cells. NSC.LMyc cells were injected intracranially (contralateral to the tumor). (A) Mouse brain section (low magnification) stained with eGFP antibody to visualize U251 glioma cells within right frontal lobe. Scale bar 1000 µm. (B, C) IHC staining of hNSC.L-Myc cells at the injection site using L-Myc polyclonal antibody. (D) IHC staining of human kidney tissue as a positive control for L-myc staining. Scale bars 100 µm.

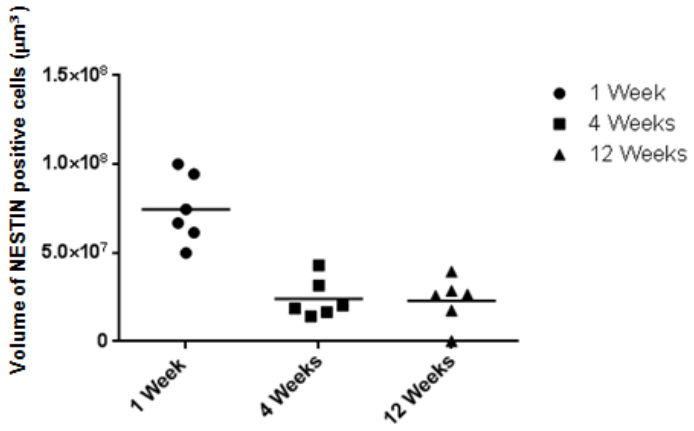

Figure S5. Human nestin expression based on 3D analysis of total volume of nestin positive cells.

NSG mice were injected intracranially with LM-NSC008 cells (right frontal lobe) and euthanized 1, 4, and 12 weeks after LM-NSC008 injection. Z-axis projection of brain sections (total 10-15 sections per brain were analyzed). Every 10^{th} section was stained with huNestin and quantification of nestin expression was performed after 1, 4 and 12 weeks of LM-NSC008 injection. Two independent animal experiments were performed (n=6) in NSG and esterase deficient ($Es1^{e}$/SCID) mice.

Table S1. DAVID Functional annotation analysis NSC008 p2 vs. NSC008 p9

Top 5 Enriched Pathway upregulated

Term	Fold Enrichment	Count	P Value
Transmission of nerve impulse	3.804615	44	7.21E-14
Synaptic transmission	3.960722	39	6.88E-13
Regulation of nervous system development	4.571122	29	3.35E-11
Cell-cell signaling	2.723758	54	4.73E-11
Regulation of neurogenesis	4.740142	26	1.92E-10

Top 5 Enriched Pathway down regulated

Term	Fold Enrichment	Count	P Value
Immune response	2.825541	49	1.08E-10
Antigen processing and presentation of peptide or polysaccharide antigen via MHC class II	14.46845	12	2.46E-10
Skeletal system development	3.866568	31	4.55E-10
Cell adhesion	2.728336	48	5.69E-10
Biological adhesion	2.724444	48	5.87E-10

Table S2. DAVID Functional annotation analysis of NSC008 and LM-NSC008 vs. differentiated LM-NSC008

Top 5 Enriched Pathway upregulated

Term	Fold Enrichment	Count	P Value
Cell adhesion	3.380163	46	8.39E-13
Biological adhesion	3.375341	46	8.70E-13
Response to wounding	3.590903	37	4.51E-11
Regulation of cell growth	5.302811	20	6.99E-09
Regulation of growth	3.921903	26	1.14E-08

Top 5 Enriched Pathway down regulated

Term	Fold Enrichment	Count	P Value
Skeletal system development	6.468944	9	6.02E-05
Cellular di-, tri-valent inorganic cation homeostasis	6.060479	6	0.002831
Sensory organ development	6.007549	6	0.00294
Prostanoid metabolic process	36.20339	3	0.002948
Prostaglandin metabolic process	36.20339	3	0.002948

Table S3. Gene expression level for SOX2, PAX6 and OCT4 genes.

Gene Symbol	LogFC	Default. set	LM-NSC008 -p2	LM-NSC008 -p12	NSC008 -p2	NSC008 -p9	LM-NSC008 -p12-Diff
SOX2	0.519168	False	140.5328	84.29378	206.0346	147.9045	103.1067
PAX6	-0.303789	False	8.208481	5.112254	3.449178	4.380321	5.294839
OCT4 (POU5F1)	6.007549	False	0.3	0.1	0.2	0.2	0.2

Table S4. Copy Number Variation (CMV) detection analysis in LM-NSC008 cells

ID	Chromosome	Start	End	Width	Number of Exons	Log2 FC	Gene
LM-NSC008-p12_vs_p2	Chr14	50808850	50811704	2855	2	-1.6103	CDKL1
LM-NSC008-p12_vs_p2	Chr3	123367818	123368009	192	2	-1.8286	MYLK

Supplemental References

Dennis, G., Jr., Sherman, B.T., Hosack, D.A., Yang, J., Gao, W., Lane, H.C. and Lempicki, R.A. (2003). DAVID: Database for Annotation, Visualization, and Integrated Discovery. Genome Biol. *4*, P3.

Koboldt, D.C., Zhang, Q., Larson, D.E., Shen, D., McLellan, M.D., Lin, L., Miller, C.A., Mardis, E.R., Ding, L. and Wilson, R.K. (2012). VarScan 2: somatic mutation and copy number alteration discovery in cancer by exome sequencing. Genome Res. *22*, 568-576.

Metz, M.Z., Gutova, M., Lacey, S.F., Abramyants, Y., Vo, T., Gilchrist, M., Tirughana, R., Ghoda, L.Y., Barish, M.E., Brown, C.E., et al. (2013). Neural stem cell-mediated delivery of irinotecan-activating carboxylesterases to glioma: implications for clinical use. Stem Cells Transl Med. *2*, 983-992.

National Institute of Allergy and Infectious Diseases (NIAID). (2016). "Database for Annotation, Visualization, and Integrated Discovery (David), v 6.7." Retrieved September 2015, from http://david.abcc.ncifcrf.gov.

Robinson, M.D., McCarthy, D.J. and Smyth, G.K. (2010). edgeR: a Bioconductor package for differential expression analysis of digital gene expression data. Bioinformatics. *26*, 139-140.

Saldanha, A.J. (2004). Java Treeview--extensible visualization of microarray data. Bioinformatics. *20*, 3246-3248.
Wilson, L.L., Tran, L., Morton, D.L. and Hoon, D.S. (2004). Detection of differentially expressed proteins in early-stage melanoma patients using SELDI-TOF mass spectrometry. Ann. N. Y. Acad. Sci. *1022*, 317-322.

Zhang, K., Chu, K., Wu, X., Gao, H., Wang, J., Yuan, Y.C., Loera, S., Ho, K., Wang, Y., Chow, W., et al. (2013). Amplification of FRS2 and activation of FGFR/FRS2 signaling pathway in high-grade liposarcoma. Cancer Res. *73*, 1298-1307.